Electrical Power and Energy Systems 142 (2022) 108125

Contents lists available at ScienceDirect

International Journal of Electrical Power and Energy Systems

journal homepage: www.elsevier.com/locate/ijepes

A communication-free active unit protection scheme for inverter dominated islanded microgrids

Md Asif Uddin Khan *, Qiteng Hong *, Agustí Egea-Àlvarez, Adam Dyśko, Campbell Booth

Department of Electronic and Electrical Engineering, University of Strathclyde, Glasgow, G1 1RD, United Kingdom

ARTICLE INFO

Keywords:
Microgrids
Inverter interfaced distributed generator (IIDG)
Inverter control and protection
Harmonic injection
Fault
Relay

ABSTRACT

Large-scale integration of different renewable energy resources introduces significant challenges to the protection of microgrids (particularly those that may operate in islanded mode), including variable and low fault levels, difficulty in operation of main and backup protection with their coordination, and bidirectional power flow during faults. As a solution to such challenges, this paper presents a novel active protection strategy for the inverter dominated islanded microgrids that coordinates protection actions with the inverter control strategy. The proposed scheme dictates specific actions from the inverter interfaced distributed generator (IIDG) controller to inject specific harmonic components into the microgrid during the fault. Relays throughout the network detect and analyse the injected harmonic components to identify the faulted section, and take appropriate isolating actions, without any requirement for relay-to-relay communication. The scheme achieves selectivity and coordination using definite time delay settings. To verify the performance of the scheme, a realistic microgrid model incorporating the proposed protection strategy has been developed in MATLAB Simulink, where a wide range of fault scenarios have been simulated with variations in fault location, type, fault resistance, line impedance, and different combinations of IIDGs (including with and without connection of a synchronous generator). Additionally, case studies using a real-time digital simulator (RTDS) platform have also been conducted to validate the performance of the proposed solution in real-time, with multiple relays implemented as hardware prototypes running on the OPAL-RT platform — thereby demonstrating the system operation in a hardware-in-the-loop (HiL) configuration. It is shown that the scheme is highly effective in detecting and isolating faults, with proper discrimination, stability and provision of backup, under all investigated scenarios.

1. Introduction

Electrical power systems are experiencing unprecedented change to meet the very challenging decarbonisation goals as part of the globally binding directives under the Paris Climate Change agreement [1]. It has been anticipated that in the future, substantial amount of inverter-based renewable generation will be integrated within power systems [2] and it is possible that certain subsystems/islands, or geographical locations of the power system will be 100% powered by inverter interfaced distributed generators (IIDGs). Microgrids solely powered by IIDGs can be extremely effective and attractive in terms of managing and coordinating inverters and their behaviours, providing access to electricity in remote locations and reducing emissions from energy systems generally [3]. An overview of several actual and implemented microgrids is presented in [4], where the majority of the projects are dominated by IIDGs. Bronsbergen holiday park in the Netherlands, Aichi project in Japan, and the CESI network in Italy are some of the examples of microgrids solely powered by power electronics-based IIDGs [4]. These IIDGs can provide extended support to the power system through the actions of the IIDG controllers, e.g. voltage support, inertia power response, etc. [5]. However, IIDGs have not properly been utilised for the purpose of supporting microgrid protection, and protection of a microgrid is often subject to significant challenges, as outlined in this paper. Therefore, this research proposes a protection scheme that takes IIDGs connected to the network under consideration and modifies the behaviour of the controllers of the IIDGs during faults to facilitate highly discriminative protection.

One of the major challenges for the proper operation of an islanded microgrid is the difficulties associated with the provision of an effective protection system [6]. Conventional distribution network protection schemes, e.g. overcurrent protection, are designed for traditional power systems, based on the assumption of relatively high fault levels supplied from an external grid and unidirectional power flow from source to

* Corresponding authors.
E-mail addresses: asif.u.khan@strath.ac.uk (M.A.U. Khan), q.hong@strath.ac.uk (Q. Hong).

https://doi.org/10.1016/j.ijepes.2022.108125
Received 12 October 2021; Received in revised form 7 February 2022; Accepted 15 March 2022
Available online 12 May 2022

consumer (and from source to fault during fault conditions). It is presumed that during the grid-connected mode in the conventional power system, standard overcurrent protection will be operational and fit for purpose. However, the fault current level in microgrids might be extremely low while operating in islanded mode [6]. Furthermore, significant integration of IIDGs increases the complexity of microgrid protection. One of the primary reasons for this is that IIDGs cannot contribute large fault current due to the limited current capacity of the inverters' semiconductor switches [7]. Additionally, the fault behaviour of the IIDG is significantly different from that of conventional synchronous generators (SGs) and can be considered as a constant current source with limited fault current magnitude [8,9]. Hence, there is a possibility that faults may not be detected by overcurrent relays during islanded operation of the microgrid. Moreover, maintaining coordination between relays using inverse definite minimum time (IDMT) characteristics could be challenging due to bidirectional power flow and restricted output current delivered by the IIDGs in the microgrid during fault conditions. Comprehensive details of challenges and maloperation of traditional overcurrent protection are discussed in [10].

Since current magnitude-based schemes i.e. overcurrent relays, reclosers, and fuses, are most probably not suitable for islanded microgrids, several new methods of detecting and locating faulted sections in such systems have been proposed by other researchers. A critical review of different protection schemes that are available in the literature is presented in [11]. For microgrid protection, [12–15] propose differential current based protection schemes. These schemes require high-bandwidth communication to exchange data among the relays to coordinate and properly detect the faults. Hence, these solutions are deemed not cost-effective nor fully reliable as the failure of communications may lead to malfunction (or non-availability of protection). Furthermore, they can be very expensive to implement. The impedance-based distance protection scheme (usually used in the transmission lines) may also not be suitable due to microgrids' inherent shorter lines with a low impedance that can be predominantly resistive in nature. A travelling wave-based protection scheme is proposed in [16], with mathematical morphology being used in the algorithm. However, the scheme with travelling wave may not be suitable for microgrid protection due to its requirement of extremely high sampling frequency for short line lengths, which are commonly seen in microgrids. Also, there is a possibility that the scheme may not differentiate between a fault and a non-faulted event due to multiple reflections and refractions of the travelling wave. Furthermore, voltage-based and total harmonic distortion-based schemes are respectively proposed by [17,18]. Fault detection using these schemes is possible, but maintaining coordination among the relays and locating the faulted section in the inverter dominated microgrids may be challenging. Adaptive protection schemes are the most researched solutions in the literature [19–21], where settings of protection schemes are modified based on prevailing conditions, e.g. network configuration, fault levels, etc. Adaptive solutions may be suitable for microgrids since the settings of the relays can be readjusted to reflect changes in the mode of operation (e.g. grid-connected mode, islanded mode). However, such schemes typically require a central controller with communication, predefined knowledge of all possible network configurations, and extensive calculation of power flows and short circuit levels at different locations in the network. Furthermore, if network changes or extensions (or new generation) are made, the overall scheme may need to be reconfigured. Hence, these solutions may not be practical for microgrid protection.

The majority of the suggested protection schemes in the literature as discussed above use passive methods, i.e. continuously monitoring parameter(s) of the network to determine fault conditions. However, only monitoring voltage or current or both may not solve the protection issues of the islanded microgrids that are powered solely by IIDGs. Therefore, different methods of active protection (i.e. intentionally injecting or modifying parameters of the network after fault detection) have also been suggested by [22–24] based on injection of non-fundamental components along with fault current. Refs. [22,23] suggest differential protection schemes that change the output frequency of at least one of the IIDGs upon detection of a fault. However, these solutions require communications functions and facilities to properly coordinate the relays, which is not cost-effective and could reduce reliability/security. Similarly, [24] proposes to inject only fifth-order harmonics through the controllers of IIDGs after detecting a fault and utilises the droop between fault current and impedance to determine the magnitude of harmonic injection. However, the scheme does not address the issue of bidirectional power flow during faults and may not fully address relay coordination issues.

Therefore, to address the technical challenges regarding the need for communications, bidirectionality, and low fault current, this paper presents a communication-free active protection method using the control strategies of the IIDGs to tackle protection issues of the islanded microgrids mostly powered by IIDGs. Ref. [25] verifies the practical use of power electronics-based inverters for sending signals (i.e. injection of harmonics) through power lines. The protection scheme presented in this paper builds upon the research concept presented in the authors' earlier publication [26], which mainly focus on the fundamental concept and preliminary investigation. In this paper, the comprehensive details of the implementation of the protection strategy, including fault detection, harmonic component selection, control and current injection, coordination between the relays, and practical consideration for application with appropriate examples, are presented, along with extensive simulation and experimental case studies under a wide range of fault scenarios to demonstrate and validate the proposed protection scheme. In this active scheme, controllers of the IIDGs intentionally modify their injected fault current based on the presence of a fault in the network. The novelty and key advantages of the scheme can be summarised as follows:

1. The proposed solution utilises multiple harmonic injections during a fault (with each of the individual IIDG injecting a specific and assigned harmonic) to identify the faulted section of the network. Injection of multiple harmonics allows the scheme to be more sensitive and can provide backup protection in networks with bidirectional power flow. As far as the authors are aware, this multiple harmonic injection has not been used by any other protection scheme.
2. Identification of the fault is independent of the fault current magnitude and the algorithm is relatively simple compared to other existing or proposed microgrids' protection schemes in technical literature.
3. The proposed solution can properly operate with a combination of synchronous generators and IIDGs, as well as, when individual generators/IIDGs are out of service.
4. The scheme does not require communication to operate properly, hence is relatively cost-effective and reliable.

The remainder of this paper is organised as follows: Section 2 explains the principle of operation of the proposed protection scheme; Section 3 presents simulation case studies obtained from Simulink, which demonstrate the effectiveness of the scheme under a wide variety of fault conditions; Section 4 illustrates the laboratory based hardware-in-the-loop (HiL) setup along with results; and finally, Section 5 concludes the paper and highlights potential future work.

2. Proposed protection scheme

2.1. Fundamental principle of operation of the proposed scheme

The proposed scheme consists of four main steps that are involved in the protection of the islanded microgrid. The first step is the fault detection, when the scheme is initiated. The fault detection is achieved

through analysis of the symmetrical components of the terminal voltage on each IIDG (explained in detail in Section 2.3). The second step is active harmonic components injection. Upon the detection of a fault by IIDGs, all connected IIDGs in the microgrid intentionally reduce output current and inject a specific predefined harmonic component which is superimposed on the output current (details of this process are discussed in Section 2.4). In the third step, all protection relays in the network analyse the harmonic content of their locally measured currents, and based on the detected harmonics, identify the faulty line in the network (refer to Section 2.5). Finally, in the fourth step, the relays in the network take appropriate actions to isolate the fault in a time coordinated manner, i.e. operating either in main or backup mode (details are discussed in Section 2.6).

2.2. IIDG control strategies

To better understand the proposed protection approach, it is helpful to talk first about the control strategies of IIDGs, as the fault behaviour of an IIDG is largely determined by its control actions. It is assumed that each generation unit in the microgrid is interfaced by a three-phase two level inverter with an LC filter as shown in Fig. 1. Several alternative inverter control strategies can be applied in practice, including real and reactive power (PQ) control, voltage and frequency (V/F) control, unity power factor control, droop control, and others [8]. Depending on their contribution to system stability, the IIDGs can be categorised either as Grid FoRming (GFR) or Grid FoLlowing (GFL) [27]. GFL provides a specific amount of power/current to the grid depending upon the set-point provided by the operator. GFR, on the other hand, acts as a

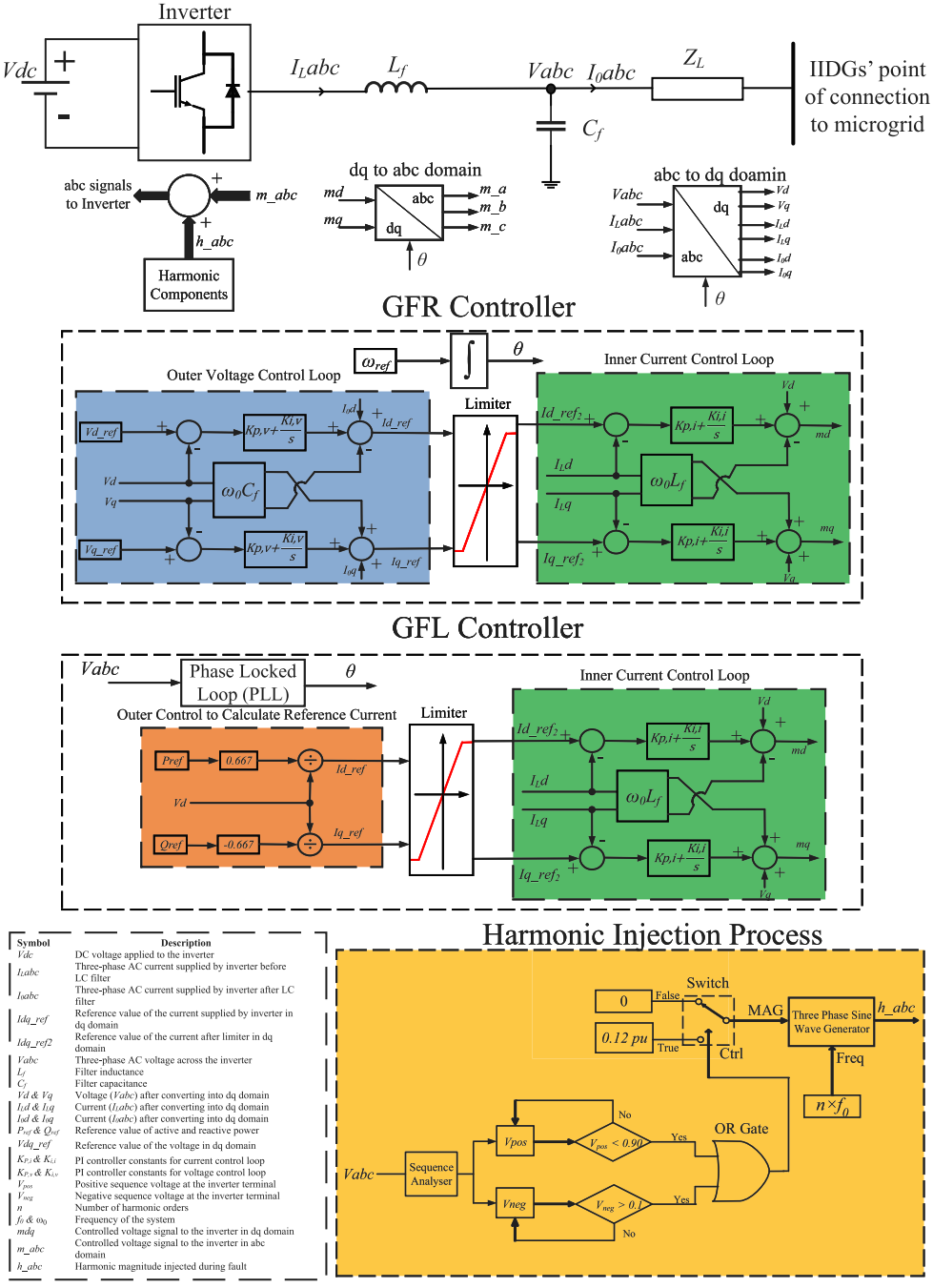

Symbol	Description
Vdc	DC voltage applied to the inverter
I_Labc	Three-phase AC current supplied by inverter before LC filter
I_0abc	Three-phase AC current supplied by inverter after LC filter
Idq_ref	Reference value of the current supplied by inverter in dq domain
Idq_ref2	Reference value of the current after limiter in dq domain
$Vabc$	Three-phase AC voltage across the inverter
L_f	Filter inductance
C_f	Filter capacitance
Vd & Vq	Voltage ($Vabc$) after converting into dq domain
I_Ld & I_Lq	Current (I_Labc) after converting into dq domain
I_0d & I_0q	Current (I_0abc) after converting into dq domain
P_{ref} & Q_{ref}	Reference value of active and reactive power
Vdq_ref	Reference value of the voltage in dq domain
$K_{P,I}$ & $K_{I,I}$	PI controller constants for current control loop
$K_{P,V}$ & $K_{I,V}$	PI controller constants for voltage control loop
V_{pos}	Positive sequence voltage at the inverter terminal
V_{neg}	Negative sequence voltage at the inverter terminal
n	Number of harmonic orders
f_0 & ω_0	Frequency of the system
mdq	Controlled voltage signal to the inverter in dq domain
m_abc	Controlled voltage signal to the inverter in abc domain
h_abc	Harmonic magnitude injected during fault

Fig. 1. Block diagram of the controllers of IIDGs.

voltage source and plays an important role in controlling voltage and frequency of the system.

Therefore, when a microgrid operates in an islanded mode, it is necessary to have at least one GFR connected to the system. In this paper, only one of the generating units is assumed to be GFR, and the rest of the generators are using GFLs. Representative diagrams for both controllers along with the proposed method for harmonic injection and fault detection are shown in Fig. 1.

The power source behind the inverter is represented by an ideal DC voltage source, and the dynamics of the different buck/boost converters and their controls (before the inverter) are not considered since the emphasis of this work is on protection of the AC side. It is assumed that the dynamics on the DC side should not have a significant impact on the AC side protection, therefore, only inverter characterisation during the fault has been taken into consideration. A detailed review of the implementation of different controllers during normal operating conditions can be found in [27]. The units controlled with GFL have a current loop that provides independent control of active and reactive power (green controller in Fig. 1), a PLL, and a PQ outer loop that provides the current references to the inner loop (marked orange in Fig. 1).

As mentioned earlier, to maintain voltage and frequency stability in the islanded microgrid, a GFR controller is used in this paper. The GFR controller has an internal current controller (marked green in Fig. 1 and a voltage controller (marked blue in Fig. 1). As the proposed protection scheme requires a fast harmonic current injection, a controller is added at the output of the current loop. It is worth mentioning that it is also possible to inject harmonics through *'dq'* current control, however, using that method of injection would be relatively slower. A detailed description of the harmonic injection controller is provided in Section 2.4. During a fault, as there will typically be a significant network voltage reduction, a large reference current will be presented to the current controller. Hence, to limit the output current of the inverter, a current limiter is used in front of the current control loop for both types of control schemes so that the reference current does not exceed the threshold. This threshold will be defined by the inverter's maximum sustained current output, which is usually around 110%–120% of its nominal output [28]. In this paper, the limit for the fundamental fault current is set to 108% after detection of a fault, leaving a margin of 12% to cater for harmonic injection and to ensure that the overall peak current remains within the 120% range. As a result, during the fault, both types of controllers and all IIDGs in the network will behave as current control sources with limited output current.

2.3. Fault detection method by IIDG

Before the injection of harmonic components from the IIDGs, the fault must initially be detected. To achieve reliable fault detection, both positive and negative sequence voltages are measured at the terminal of the IIDGs through the controller of the inverter. The process can be explained with reference to Fig. 1 (harmonic injection process). The threshold for positive sequence under-voltage element is set to 0.9 pu (i.e. the voltage lower than the threshold sets the output state to high) and the negative sequence over-voltage threshold is 0.1 pu (i.e. the voltage above the threshold triggers the element). Balanced faults will be detected by the positive sequence voltage, while negative sequence element will indicate unbalanced faults. Either threshold being violated will trigger subsequent steps of the scheme. The positive and negative sequence thresholds can both be varied.

To cater for non-fault transient under-voltage or phase imbalance conditions, an intentional time delay of 100 ms is included in each of the relays before any operation is initiated. This delay results in longer protection operating times, but it should be noted that fault clearance time requirements in an islanded microgrid are typically not very stringent due to the relatively low fault levels and thus limited impact on electrical equipment. Furthermore, since the vast majority faults on microgrids are unbalanced in nature, negative sequence voltage analysis will safeguard the scheme's stability during non-faulted conditions. Furthermore, to coordinate the scheme's setting with the existing GB grid code [29] where the minimum voltage level for normal operation is 0.9 pu, the relay threshold is set accordingly. Finally, the under-voltage and unbalance threshold settings and time delays, can all be configured to accommodate specific system conditions and/or regulation.

In this work, systematic simulation has been conducted, where a range of resistive faults with increasing value of fault resistance have been applied at different locations. Furthermore, sensitivity analysis has been performed, which shows that with the assumed voltage settings (i.e. 0.9 pu), the scheme is capable of providing a very good level of dependability to high impedance faults, i.e. the scheme can operate correctly with fault resistances up to a limit of 60 Ω, which can be considered as high fault impedance in a practical 11 kV system.

Upon the detection of fault or triggering of the scheme, harmonic components are injected. It should be noted that in normal operation (when there is no fault) no harmonics are injected and hence h_abc is set to zero. When a fault is detected a specific magnitude of a specific harmonic component will be injected by each generator — the magnitude and nature of the harmonics injected will be clearly discernible from normal background noise and power quality related harmonics.

2.4. IIDG injection of harmonic components

Two main criteria, i.e. the order and the magnitude of the harmonics, must be addressed to ensure appropriate injection of harmonic components during fault conditions. Theoretically, it is possible to inject any order of harmonics. However, considering the practical aspects, in the proposed scheme, lower order harmonics (2^{nd}, 3^{rd} and 4^{th}) are used. Harmonic components higher than 10 are not typically considered, as the resonant frequency of the LC filter is typically between 10 times of the grid frequency and half of the converter switching frequency [30]. Therefore, limiting the injected harmonics to the 10^{th} order ensures that no unnecessary filtering of the protection related frequencies occurs. It should also be noted that it is not essential for all the IIDGs in the network to inject harmonics. Injection from IIDGs with relatively high capacity is sufficient as discussed in detail in Section 2.7. Therefore, in the proposed scheme, injection of harmonics higher than 10 can be realistically avoided. Finally, inter-harmonics or other specific frequencies could be used (below the 10^{th} harmonic) if a relatively high number of protected lines/circuits with IIDGs are present in a particular microgrid.

In terms of harmonic magnitude, currently, there is no requirement or limitation on the magnitude of harmonics during faults from a regulatory/system operation perspective. However, according to IEEE standard 519 [31], during the normal operating condition, the maximum allowable magnitude of harmonics (low order) is 4% of the maximum load current. Therefore, to differentiate harmonics during normal and fault conditions, in this proposed scheme, the magnitude of harmonics is set to be 10% of the fault current (i.e. 0.12 pu in terms of rated current as fault current magnitude is assumed to be 1.2 pu). Again, it is important to mention that the proposed scheme will not inject harmonic components continuously, but only for a short time, when a fault is detected by the inverters' controllers. Therefore, the harmonic injection will not have a large impact on the loads, transformers, fault ride-through (FRT) requirements of the IIDGs, or power quality. Regarding FRT, it is assumed that the inverters will remain connected during a fault following grid code requirements. The fundamental output current will be reduced only marginally, i.e. by 10% of the rated current. This 10% headroom is then used for harmonic injection. Therefore, the proposed solution will not be detrimental to the FRT requirements of inverters. During faults, loads in the vicinity of the fault may be experiencing significant under-voltages anyway, so any relatively small harmonic distortion of the current will not have a significant impact.

2.5. Detection and identification of faulted line section by relays

In this research, two circuit breakers (CBs) for each section of the line is used (as demonstrated in Fig. 6) and hence, in this protection scheme, there are two relays; one at each end of every section of the line. These relays are categorised into two groups — forward group relay (FGR) and backward group relay (BGR). The relays upstream of each line (left hand side) are FGRs, and the relays downstream of each line (right hand side) are BGRs.

For traditional passive grid-connected radial systems, normally only one CB at the upstream end (i.e. the end that would be supplying fault current) of the line is used since there is no contribution of fault current from the downstream system. However, in future microgrids relying solely on distributed generation at many locations throughout the network, it will be necessary to use two CBs in a single interconnecting line due to the presence of multiple IIDGs in the microgrid and bidirectional power flow during both normal and fault conditions. Therefore, even if a fault is detected by a relay at one end, there is a chance that current will be fed to the fault from the downstream position. In that case, generation will be lost and supply to the other connected loads may also be compromised. It is important to note that, in the proposed scheme, no communication between the relays (FGRs and BGRs) is required to achieve protection coordination among the relays, which is beneficial. In grid-connected mode, conventional protection and CB arrangements may be sufficient (but this protection scheme could still also be in operation to interrupt/isolate IIDGs).

To identify the faulted line section, FGRs analyse the injected harmonic components from the upstream IIDGs, while the BGRs analyse harmonic components injected by the downstream IIDGs. The algorithm for fault detection of the proposed solution is presented in Fig. 2. The harmonic component threshold for relay operation must be greater than 0.04 pu since as mentioned earlier, during normal operating conditions, the accepted range of lower-order harmonic presence in an 11 kV system is 4% [30]. Therefore, in this research, the threshold for the relays in the network is set to 0.08 pu which provides sufficient headroom to detect a fault and non-faulted situation. Relays can analyse the harmonics of the current through (1), where, k is the harmonic number (e.g. $k = 1$ means fundamental; $k = 2$ is 2nd harmonic, etc.), I_k is calculated harmonic current magnitude, $I(t)$ is the measured current fed to the relay, f_0 is the fundamental frequency of 50 Hz, and T is the period of the input current (inverse of the fundamental frequency, f_0). The block diagram of the implementation of the relay is shown in Fig. 3, where, measured current, $I(t)$, fundamental frequency, f_0, a matrix of harmonics, $k = 2; 3; 4;$ etc., and threshold of the harmonic magnitude, I_{th} will be given as input and the relay will provide the tripping signal as output.

$$I_k = 2f_0\sqrt{\left(\int_{t-T}^{t} I(t)\sin(2\pi k f_0 t)\,dt\right)^2 + \left(\int_{t-T}^{t} I(t)\cos(2\pi k f_0 t)\,dt\right)^2} \quad (1)$$

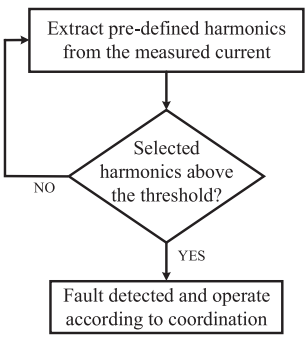

Fig. 2. Relay tripping logic.

2.6. Relay coordination

The proposed method utilises definite time characteristics to coordinate the relays. The operating time settings for the FGRs are set in a way that the most downstream relays operate faster and the most upstream relays operate slower, with a constant time grading being applied between two consecutive relays. On the contrary, the BGRs are set opposite to the FGRs, i.e. the most upstream relays will operate the fastest, and downstream will operate slower with a constant time difference.

Inherently longer operating times for certain faults is the major drawback of using definite time delay coordination, especially in the case of grid-connected operation where fault current is relatively high and the potential for damage with sustained faults on the system increases. However, fault currents are significantly lower during islanded mode; accordingly, the slow operation should be more tolerable. Furthermore, during an upstream fault, the current contribution from the majority of the IIDGs is quickly eliminated due to the fast operation of the BGRs. Also, due to restricted output currents of IIDGs during fault, the fault current magnitudes in the islanded microgrid will be limited and is not expected to vary significantly with the variation of fault location. Therefore, the use of IDMT characteristic is unlikely to provide a reduction in protection operation times, as it would otherwise be the case in a distribution system with higher fault level (i.e. grid-connected). Additionally, the use of communication to coordinate the relays can be costly and may prove unreliable. Thus, in the case of islanded microgrid protection, definite time characteristic was considered most suitable. An additional benefit of such time grading approach is the inherent provision of backup protection functionality.

2.7. Protection operation example and practical considerations

To better understand the operation of the proposed scheme a simple fault scenario is presented in this section. Fig. 4 represents a small section of a microgrid with IIDG connected at each end of the line, where both IIDGs, i.e. $IIDG_1$ and $IIDG_2$ inject different order harmonics I_{H1} and I_{H2} respectively, after detecting the presence of a fault. Faults are initially identified by IIDGs using the sequence components of the measured terminal voltage. According to the proposed scheme, during a fault inside the protected section (F_1), relay R_1 will detect I_{H1}, and relay R_2 will detect I_{H2}, and both relays operate accordingly to isolate the faulted section. In the case of a fault outside the protected section, e.g. fault F_2 as shown in Fig. 4, $IIDG_1$ and $IIDG_2$ both will inject harmonic components towards the relay R_3. Therefore, relay R_2 will not detect the harmonic component I_{H2} and will not issue a trip, however, relay R_1 can still detect the fault and can be operated as backup protection, i.e. R_3 operating fast and R_1 with a time delay.

To further clarify the key assumptions and additional practical considerations of the proposed scheme the following points are included:

1. All of the connected IIDGs in the network inject harmonic components during a fault, with IIDGs connected to neighbouring buses injecting different order harmonics. However, it is also possible to coordinate the relays (both detecting and identifying the faulted section) through the harmonic injection from a single IIDG, i.e. injection of only one harmonic component as shown in the results of the different combination of IIDG location (refer to Section 3.6). Injection of harmonic components from all IIDGs makes the scheme more reliable in case any IIDG(s) in the network being out of service. Also, in circumstances where multiple IIDGs connected to a single bus, all of them might inject the same harmonic component into the system, or a single IIDG could be selected for harmonic injection during the fault. Typically, a relatively large-rated generator, expected to be constantly connected to the network, would be most suitable for this. In the future, large scale storage units may become

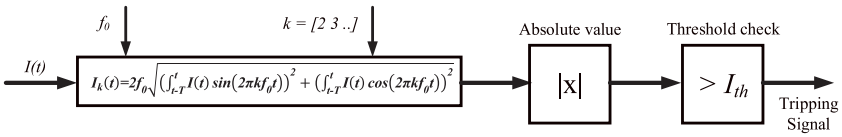

Fig. 3. Generic block diagram of the proposed scheme's relay.

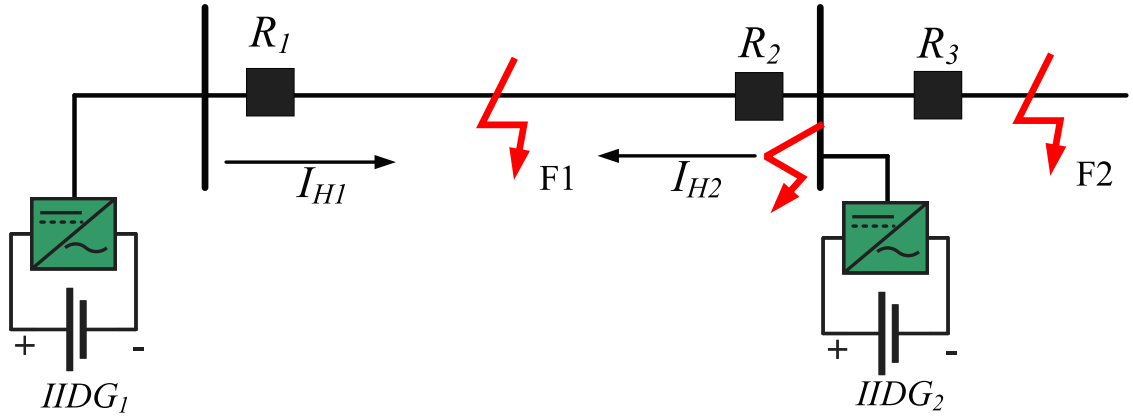

Fig. 4. Single section of a microgrid with two IIDGs.

widely accessible in microgrids, and it could be convenient to inject harmonic components using these units (assuming they are never at zero state of charge) with the proposed solution since they should always remain connected to the network, whether in charging/discharging or "floating" mode.

2. The proposed solution is suitable for the protection of microgrids with both radial and meshed architectures. However, to protect meshed networks an additional arrangement is needed. It is proposed that the scheme would be equipped with fast-acting sectionalisers/isolators (which could be triggered by overcurrent or under-voltage element), connected to a suitable point in the network (e.g. the "mid-point" or where a normally open point would be located in typical distribution networks). When a fault occurs on the network (at any location), the isolator would operate quickly (with a delay of around 0.05 s), thereby separating the network into radial sub-networks, and then the relays can operate on the faulted section of the radial networks as explained in this paper. An example arrangement of the proposed scheme to protect a meshed network can be explained with the aid of Fig. 5. A sectionaliser, R_{sec} is installed at the interconnection point between Busses 1 and 3. When there is a fault in the network (at any location), R_{sec} is tripped very quickly (with a delay of around 0.05 s) and other relays will operate as they would for a radial network, as the network will have been split rapidly following initial fault detection. Paper [32] presents a fast mechanical switch that operates very quickly within only a few milliseconds and this could be utilised in conjunction with the proposed scheme. Even if the sectionaliser/isolator is not capable of operating extremely quickly, the operating times of the proposed scheme could be extended to cater for this. Given that fault levels in islanded microgrids may be relatively low, it is probable that a relatively low interrupting rating would be sufficient for such sectionaliser/isolator. It is also worth noting that many distribution networks and microgrids are not operated in a meshed fashion [4] due to the complexity of protection and the requirement to isolate more customers for every fault, so it is anticipated that the proposed scheme would mainly be implemented in radial networks.
3. The scheme is proposed for islanded microgrids (which is assumed to be the predominant mode of operation) where the relays do not need to communicate with each other to detect a fault and coordinate properly, and it has been assumed that a separate method of detecting islanding is in place, i.e. this scheme does not detect islanded mode but is assumed to be operational only when the system is islanded. Therefore, it has been assumed that an overall microgrid management system (which would only require very simple non-continuous signalling-based communications) is available, which is typically the case in existing microgrids, to activate/disconnect the protection scheme depending on the microgrid's mode of operation.

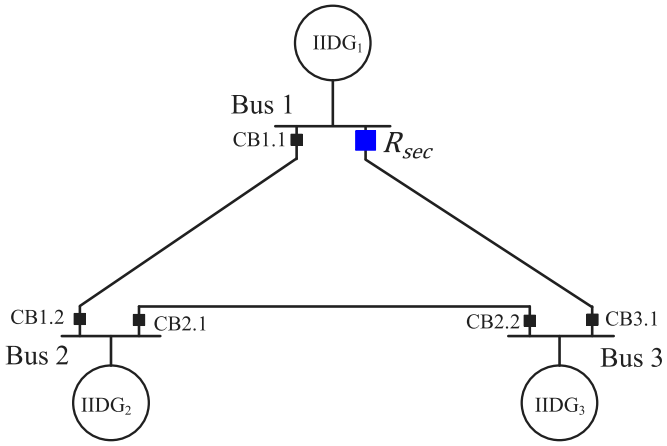

Fig. 5. Meshed network protection.

4. A fault between FGR and BGR, e.g. fault between relay, R_2 and R_3 in Fig. 4 is assumed to be an internal busbar fault. Therefore, to clear the fault at such a location, it is assumed that a separate protection unit is already available at ring main unit (RMU)/busbar. If the fault is not cleared by the RMU/busbar protection, the proposed protection scheme still can detect such faults, e.g. in the case shown in Fig. 4, relay R_1 will detect the fault and operate accordingly as a backup.

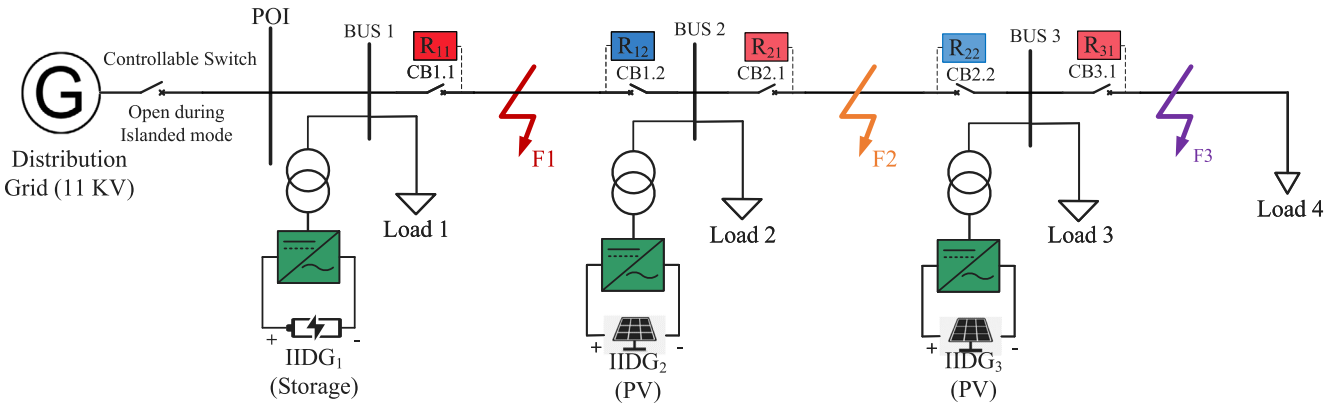

Fig. 6. Model of the test microgrid for proposed protection scheme's verification.

Table 1
Parameters for the microgrid model.

Simulation parameters	Description and symbol	Values
Frequency	f_0	50 Hz
AC grid and base voltage	V or V_{base}	11 kV
Line impedance	Z_{Line}	0.0543+j0.0495 Ω/km
Line length	Line between POI and Bus 1, l_{01} Line between Bus 1 and Bus 2, l_{12} Line between Bus 2 and Bus 3, l_{23} Line after Bus 3, l_3	0.5 km 1.8 km 2 km 1 km
IIDG rating and base power	For each generator, S_{base}	500 kVA
Reference value of IIDGs	$IIDG_1$ $IIDG_2$ $IIDG_3$	400 kVA 100 kVA 50 kVA
LC filter	L and C	43 μH and 1.88 mF
Inverter's DC voltage	V_{dc}	500 V
Inner and outer control loop	Voltage loop proportional gain, $K_{p,v}$ Voltage loop integral gain, $K_{i,v}$ Current loop proportional gain, $K_{p,i}$ Current loop integral gain, $K_{i,i}$	2 20 0.3 10
Load rating	$Load_1$ $Load_2$ $Load_3$ $Load_4$ Total Load	200 kVA 200 kVA 100 kVA 50 kVA 550 kVA

3. Simulation based performance validation of the proposed scheme

To verify the effectiveness and analyse the performance of the proposed solution, several fault scenarios have been simulated in the microgrid shown in Fig. 6. The microgrid model is developed in MATLAB Simulink in accordance with IEEE2030.7 [33].

3.1. Overview of the microgrid model

As can be seen from Fig. 6, the microgrid is designed in a way that it can be operated either in grid-connected mode or islanded mode, through the controllable switch at the point of interconnection (POI) to the 11 kV distribution grid. However, since this research focuses only on the protection of islanded microgrids, during the simulations, the grid will always remain disconnected. There are three loads and three IIDGs connected to the network; each bus has one load and one IIDG. The rating of each IIDG is assumed 500 kVA. $IIDG_1$ is the GFR, and therefore, controlling islanded microgrid's voltage and frequency. $IIDG_2$ and $IIDG_3$ both are the GFLs, and will provide a constant amount of active and reactive power to the microgrid. Line parameters for the modelled microgrid are designed based on real distribution lines as surveyed in [32], and details of the IIDGs are shown in Table 1.

Table 2
Injected harmonic components from IIDGs.

Generator	Injected harmonic components
$IIDG_1$	2^{nd} Harmonic (I_{HC2})
$IIDG_2$	3^{rd} Harmonic (I_{HC3})
$IIDG_3$	4^{th} Harmonic (I_{HC4})

3.1.1. Selection of harmonics

In this paper, for three IIDGs as presented in Fig. 6, three different order harmonics are injected into the network during fault conditions. The injected order of harmonic components by the IIDGs for the microgrid shown in Fig. 6 is presented in Table 2. As shown in Table 2, upon detection of a fault, $IIDG_1$ injects 2^{nd} harmonic (I_{HC2}), $IIDG_2$ injects 3^{rd} harmonic (I_{HC3}) and $IIDG_3$ injects 4^{th} harmonic (I_{HC4}). Current supply from each IIDG during both normal and fault condition is presented in Fig. 7. Also, the magnitude of fundamental and harmonic components is shown in the same figure. As can be seen from Fig. 7, after a three-phase bolted fault at F_3 (at 0.5 s) each IIDG injects its respective harmonic component and peak of the fault current remain within the 120% of the rated capacity.

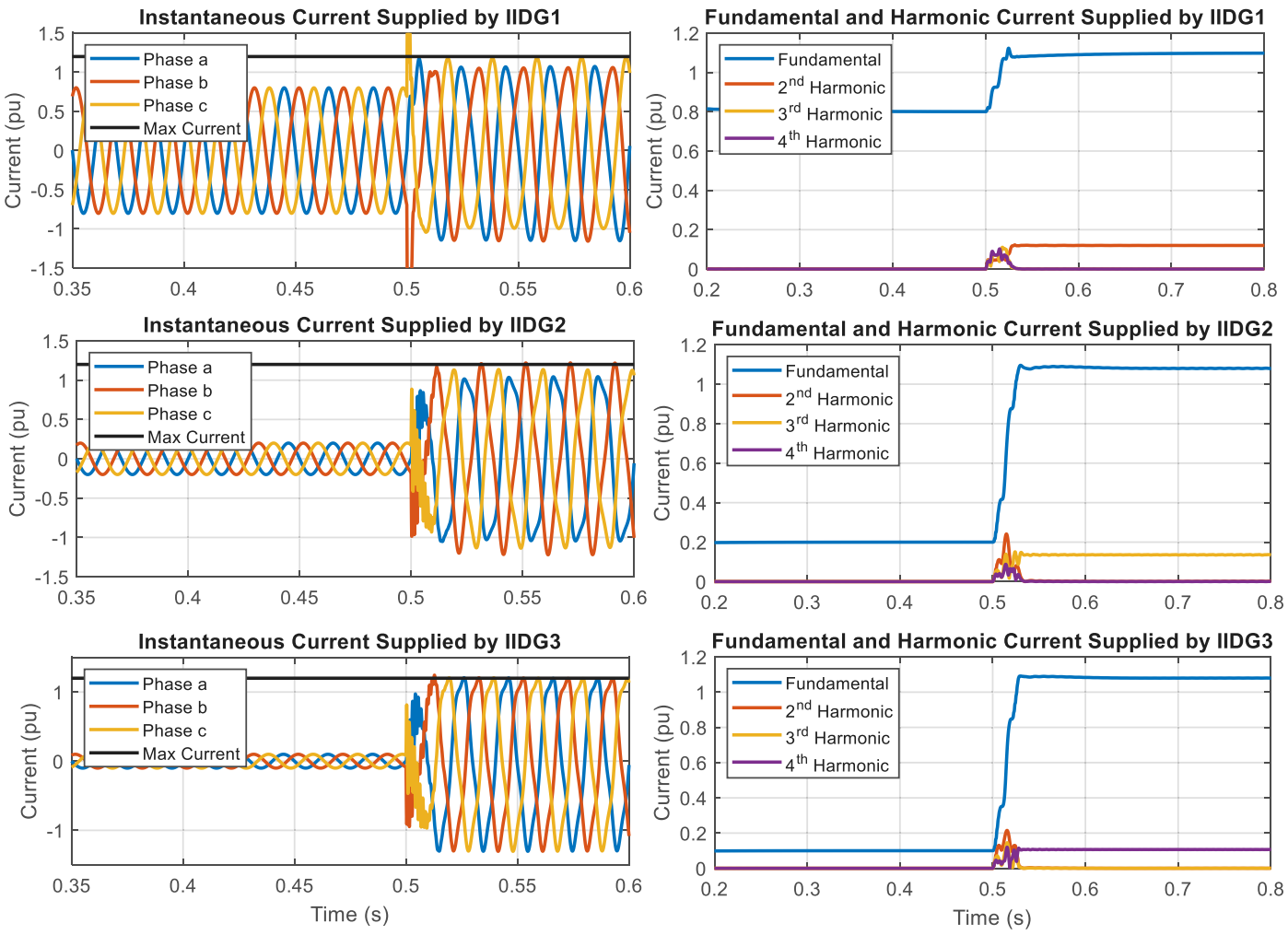

Fig. 7. Harmonic and fundamental current measurements from the IIDGs.

Table 3
Relay settings.

Relay	Operating time (s)	Fault detection condition
R_{11}	0.3	I_{HC2}
R_{21}	0.2	I_{HC2} or I_{HC3}
R_{31}	0.1	I_{HC2} or I_{HC3} or I_{HC4}
R_{12}	0.1	I_{HC3} or I_{HC4}
R_{22}	0.2	I_{HC4}

3.1.2. Relay settings

To identify and isolate faults, CBs and proposed relays are installed at both ends of each line section. The relays are split into two groups: FGRs (R_{11}, R_{21} and R_{31}) and BGRs (R_{12} and R_{22}), with each relay having an associated CB.

From Fig. 6, it is evident that R_{11} analyses injected components from the $IIDG_1$ (I_{HC2}), R_{21} analyses components from $IIDG_1$ (I_{HC2}) and $IIDG_2$ (I_{HC3}), and R_{31} checks the components of I_{HC2}, I_{HC3} and I_{HC4}. In the case of BGRs, R_{21} analyses components injected by the downstream IIDGs, $IIDG_2$ (I_{HC3}) and $IIDG_3$ (I_{HC4}), and R_{22} analyses the injected component from $IIDG_3$ (I_{HC4}). The decision making through analysed components and tripping time for all relays are summarised in Table 3.

Different scenarios by varying fault types, location and impedance are simulated for the validation of the proposed scheme and results for each scenario are described in the following subsections.

3.2. Balanced faults

Three-phase balanced faults (at locations F_1, F_2 and F_3) have been simulated as shown in Fig. 6 and the operation of the relays (in terms of tripping outputs) have been recorded with measured fundamental and harmonic currents. In order to observe the operation of backup protection functionality, none of the faults has been removed from the system and the CBs have not been opened in response to main protection signals so that a full picture of the subsequent (main and backup) response of the entire protection system can be observed and evaluated.

While the detailed results are presented for one of the fault cases only, all results in terms of operating times of the relays are summarised in Table 4. For a fault between Bus 2 and Bus 3, F_2, the inputs (fundamental current magnitude along with harmonics) and outputs of both FGRs and BGRs are presented in Figs. 8 and 9. The fault is applied at 0.5 s. From the results, the following observations can be made regarding FGR and BGR responses.

For FGRs:

- R_{31} does not detect any harmonic, so remains inactive.
- R_{21} detects 2^{nd} and 3^{rd} harmonics (I_{HC2} and I_{HC3}), so should trip at 0.7 s (i.e. 0.2 s after fault inception).
- R_{11} detects 2nd harmonic (I_{HC2}), so would trip at 0.8 s (0.3 s after fault inception) as a backup.

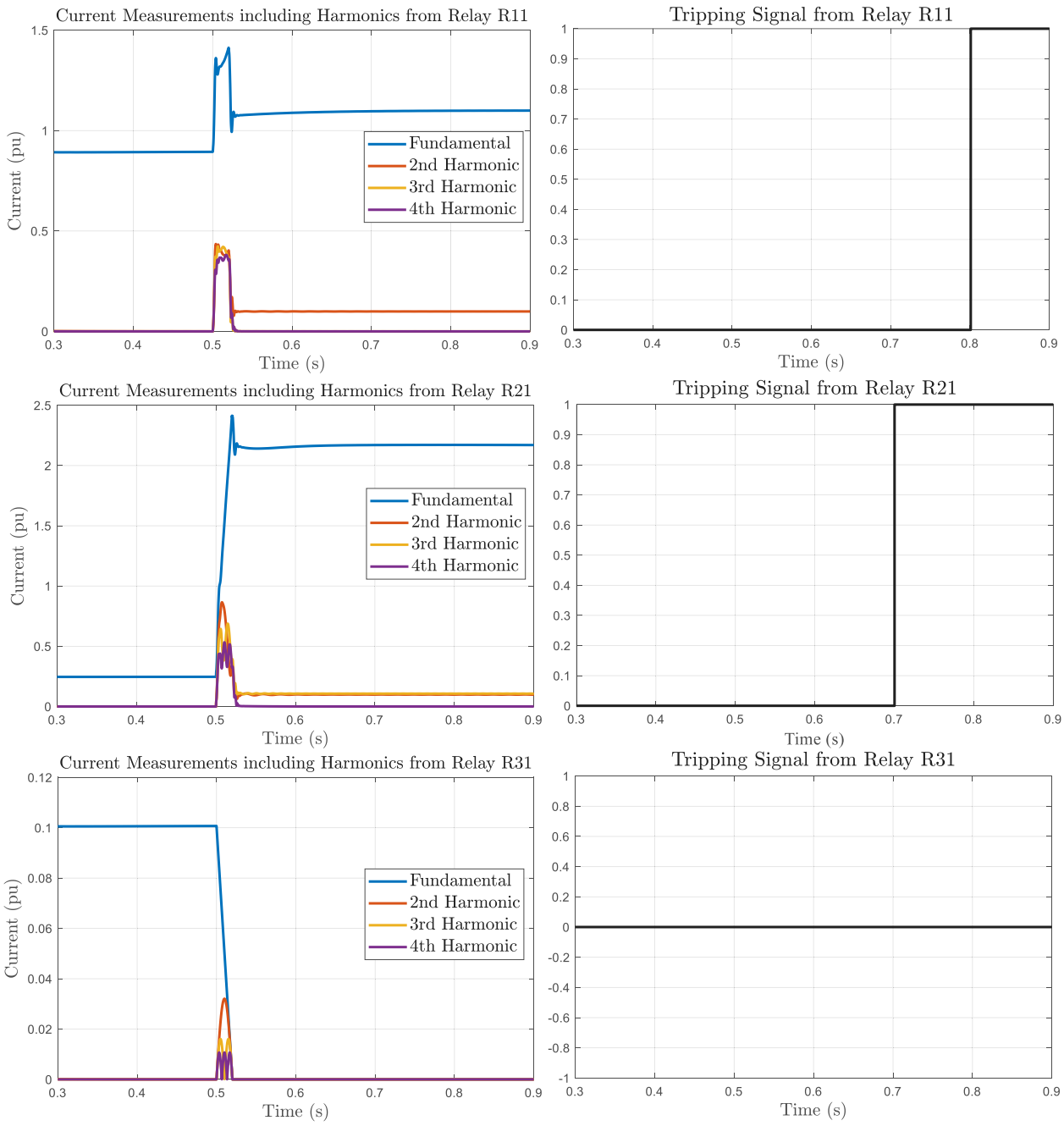

Fig. 8. FGRs' input: current measurements with harmonics; and outputs: tripping signals for fault, F_2.

For BGRs:

- R_{12} detects 2nd harmonic so remains inactive.
- R_{22} detects 4th harmonic component (I_{HC4}), so trips at 0.6 s (0.2 s after the fault).

3.3. Unbalanced faults

The performance of the system for two types of unbalanced faults is reported in this section: phase to earth fault and phase to phase. Similar to the previous case, faults have been applied at different locations of the microgrid and cases 4–21 in Table 4 show the successful operation of the proposed scheme for all unbalanced faults.

3.4. High impedance faults (HIFs)

The fault resistance at F_3 has been varied to test HIF performance. Two different types of faults have been simulated at this location, a balanced three-phase to earth fault and a single phase to earth fault (A-G). Cases 22–33 of Table 4 show the relay tripping times for different fault impedances. It can be observed that the scheme can properly detect and coordinate for HIFs with fault impedances of up to 20 Ω for single-phase to ground faults, and for three-phase faults, the maximum value of fault resistance that can be catered for is 60 Ω. Fault can be detected by the relays for resistances beyond the mentioned value for single-phase to earth faults, however, coordination among the relays may be compromised.

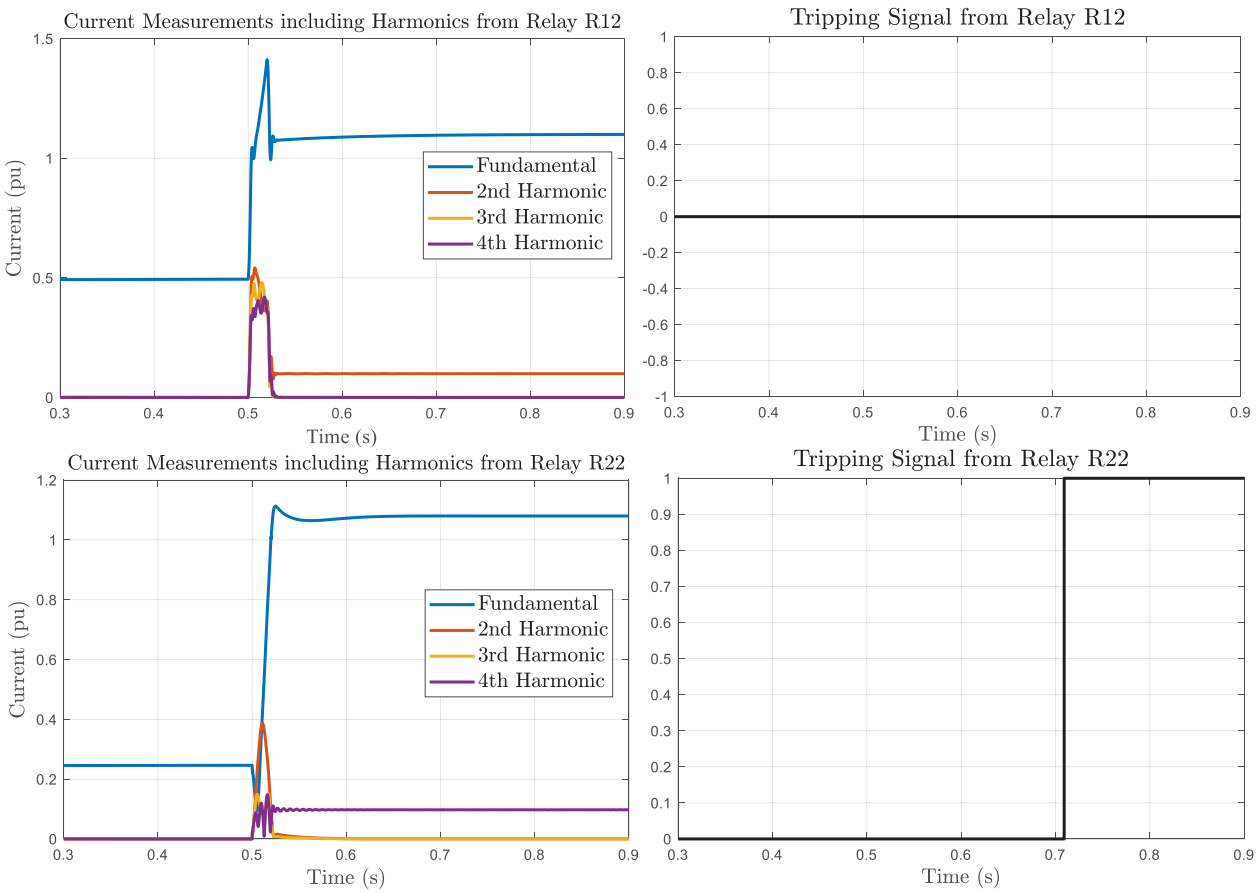

Fig. 9. BGRs' input: current measurements with harmonics; and outputs: tripping signals for fault, F_2.

3.5. Different line length/impedance

The maximum line length of the tested microgrid is 5.3 km and the scheme can operate properly within this boundary. In this section, the capability of the scheme for longer line lengths is tested and the output is shown in Table 4. From the results for cases 34–40, it can be concluded that the scheme works perfectly for the lines where lengths of more than 100 km (which is very high for microgrid). However, the injected components become highly unstable while line length is equal to or more than 144.5 km, therefore, even though the scheme is working, it is been considered the scheme is limited up to this line length.

3.6. Different combination of IIDG locations

Three different scenarios have been tested for a three-phase fault at F_3 to validate scheme operation for different IIDG locations. Initially, only IIDG_1 is connected and the response, as shown in Table 5, verifies correct operation. Secondly, IIDG_1 and IIDG_2 are connected and finally, IIDG_1 and IIDG_3 are connected. For all cases, the scheme operates correctly in terms of both main and backup responses.

3.7. Combination of IIDGs and synchronous generator (SG)

In this simulation, IIDG_2 in Fig. 6, is replaced with a conventional SG model with the same rated capacity of 500 kVA to verify the operation of the proposed solution when mixed generation comprising SGs and IIDGs is used in the microgrid. The fault current supplied by the SG during a fault at F_2 is shown in Fig. 10, along with the harmonic and fundamental currents measured by relays R_{21} and R_{22}. As can be seen in the figure, a fault is initiated at 0.5 s and in response, the SG has injected a fault current that is 3.6 times the value of the rated current. However, this high fault current does not have a negative impact on the harmonic injection through the IIDGs, nor does it limit the ability of the harmonics to be detected and measured by the relay. Therefore, the proposed scheme can successfully identify the faulted section and can take necessary actions to isolate the fault from the network. However, it is necessary to mention that, to identify the faulted section from both ends relays, injection is required from both "ends" of the network. Hence, the location of SGs would have to be between two IIDGs, which could limit applicability in some specific configurations.

4. Real time hardware-in-the-loop test and results

To further validate the performance of the proposed protection scheme, an HiL experimental configuration has been established as shown in Fig. 11, and case studies have been executed using this arrangement in the laboratory environment. The microgrid shown in Fig. 6 is implemented in the real-time digital simulator (RTDS) [34] to emulate the real-time dynamics of the microgrid during both normal and fault conditions. The input currents of the relays R_{21} and R_{22} are sent to the OPAL-RT [35] through the Giga-Transceiver Analogue Output (GTAO) card within the RTDS. Within the OPAL-RT system, relays, R_{21} and R_{22} are implemented and the software operates in real time. The relays analyse the measurement signals received from the RTDS using the algorithm and relay logic presented in Figs. 2 and 3. Any tripping signals from the relays are fed back to the RTDS using the Giga-Transceiver Digital Input (GTDI) card as the inputs to the simulation, closing the real-time simulation loop.

As shown in Fig. 6, three-phase faults have been simulated at different locations throughout the microgrid network. The measured harmonic components and tripping signals of the relays (R_{21} and R_{22})

Table 4
Verification of the proposed solution under different fault simulations.

Case No.	Fault location	Fault type	Fault impedance (Ω)	Fault distance from Grid (km)	Fault clearing time (s)					Correct operation?
					CB1.1	CB1.2	CB2.1	CB2.2	CB3.1	
1	F_3	ABC	0.1	5.3	0.8	–	0.7	–	0.6	Yes
2	F_2	ABC	0.1	3.3	0.8	–	0.7	0.7	–	Yes
3	F_1	ABC	0.1	1.4	0.8	0.6	–	0.7	–	Yes
4	F_3	A-G	0.1	5.3	0.77	–	0.7	–	0.6	Yes
5	F_3	B-G	0.1	5.3	0.81	–	0.7	–	0.6	Yes
6	F_3	C-G	0.1	5.3	0.81	–	0.7	–	0.6	Yes
7	F_3	A-B	0.1	5.3	0.77	–	0.7	–	0.6	Yes
8	F_3	B-C	0.1	5.3	0.84	–	0.7	–	0.6	Yes
9	F_3	C-A	0.1	5.3	0.83	–	0.7	–	0.6	Yes
10	F_2	A-G	0.1	3.3	0.77	–	0.7	0.71	–	Yes
11	F_2	B-G	0.1	3.3	0.81	–	0.7	0.74	–	Yes
12	F_2	C-G	0.1	3.3	0.81	–	0.7	0.71	–	Yes
13	F_2	A-B	0.1	3.3	0.77	–	0.7	0.74	–	Yes
14	F_2	B-C	0.1	3.3	0.84	–	0.7	0.75	–	Yes
15	F_2	C-A	0.1	3.3	0.83	–	0.7	0.73	–	Yes
16	F_1	A-G	0.1	1.4	0.83	0.64	–	0.72	–	Yes
17	F_1	B-G	0.1	1.4	0.82	0.61	–	0.71	–	Yes
18	F_1	C-G	0.1	1.4	0.77	0.62	–	0.71	–	Yes
19	F_1	A-B	0.1	1.4	0.77	0.62	–	0.73	–	Yes
20	F_1	B-C	0.1	1.4	0.77	0.66	–	0.76	–	Yes
21	F_1	C-A	0.1	1.4	0.77	0.64	–	0.74	–	Yes
22	F_3	ABC	1	5.3	0.8	–	0.7	–	0.6	Yes
23	F_3	ABC	5	5.3	0.79	–	0.72	–	0.62	Yes
24	F_3	ABC	10	5.3	0.79	–	0.72	–	0.62	Yes
25	F_3	ABC	15	5.3	0.79	–	0.72	–	0.64	Yes
26	F_3	ABC	20	5.3	0.79	–	0.72	–	0.64	Yes
27	F_3	ABC	30	5.3	0.79	–	0.72	–	0.64	Yes
28	F_3	ABC	50	5.3	0.79	–	0.73	–	0.64	Yes
29	F_3	ABC	66	5.3	0.79	–	0.73	–	0.73	Yes
30	F_3	A-G	1	5.3	0.81	–	0.7	–	0.6	Yes
31	F_3	A-G	10	5.3	0.81	–	0.7	–	0.6	Yes
32	F_3	A-G	15	5.3	0.78	–	0.75	–	0.64	Yes
33	F_3	A-G	20	5.3	0.81	0.76	0.92	–	0.64	No
34	F_3	ABC	0.1	14.3	0.8	–	0.7	–	0.6	Yes
35	F_3	ABC	0.1	24.3	0.8	–	0.7	–	0.6	Yes
36	F_3	ABC	0.1	34.3	0.8	–	0.71	–	0.6	Yes
37	F_3	ABC	0.1	44.3	0.8	–	0.71	–	0.6	Yes
38	F_3	ABC	0.1	54.3	0.8	–	0.71	–	0.62	Yes
39	F_3	ABC	0.1	64.3	0.8	–	0.71	–	0.62	Yes
40	F_3	ABC	0.1	144.3	0.82	–	0.71	–	0.62	No

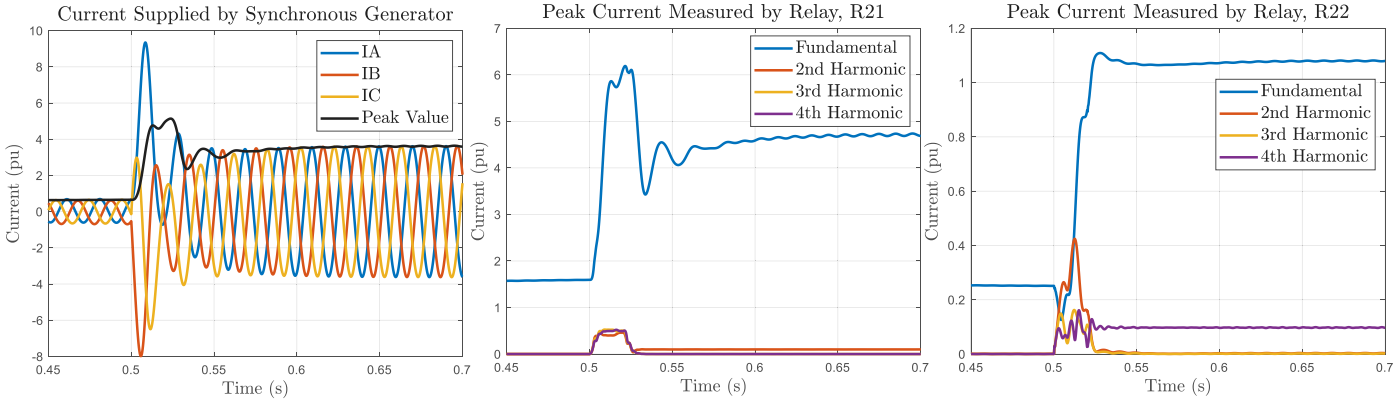

Fig. 10. Simulation results for combination of IIDGs and SG.

in response to simulated faults at three selected locations are shown in Figs. 12–14. As can be seen from Fig. 13, a fault has been initiated at 0.4 s and both relays issue a tripping signal at 0.6 s (0.2 s after the fault inception) for a fault at location F_2. For a fault at F_1, only relay R_{22} issues a tripping signal at 0.6 s (0.2 s after the fault inception), under the assumption that relay R_{12} (which is not included in the HiL arrangement) has not issued any tripping signal at 0.1 s. Finally, for a fault at location F_3, relay R_{21} issues a tripping signal at 0.6 s, again under the assumption that R_{31} (which is not included in the HiL arrangement) has not issued any tripping signal at 0.1 s.

5. Conclusion and future work

This paper has presented a novel communication-free active unit protection scheme to detect and isolate faults to address protection

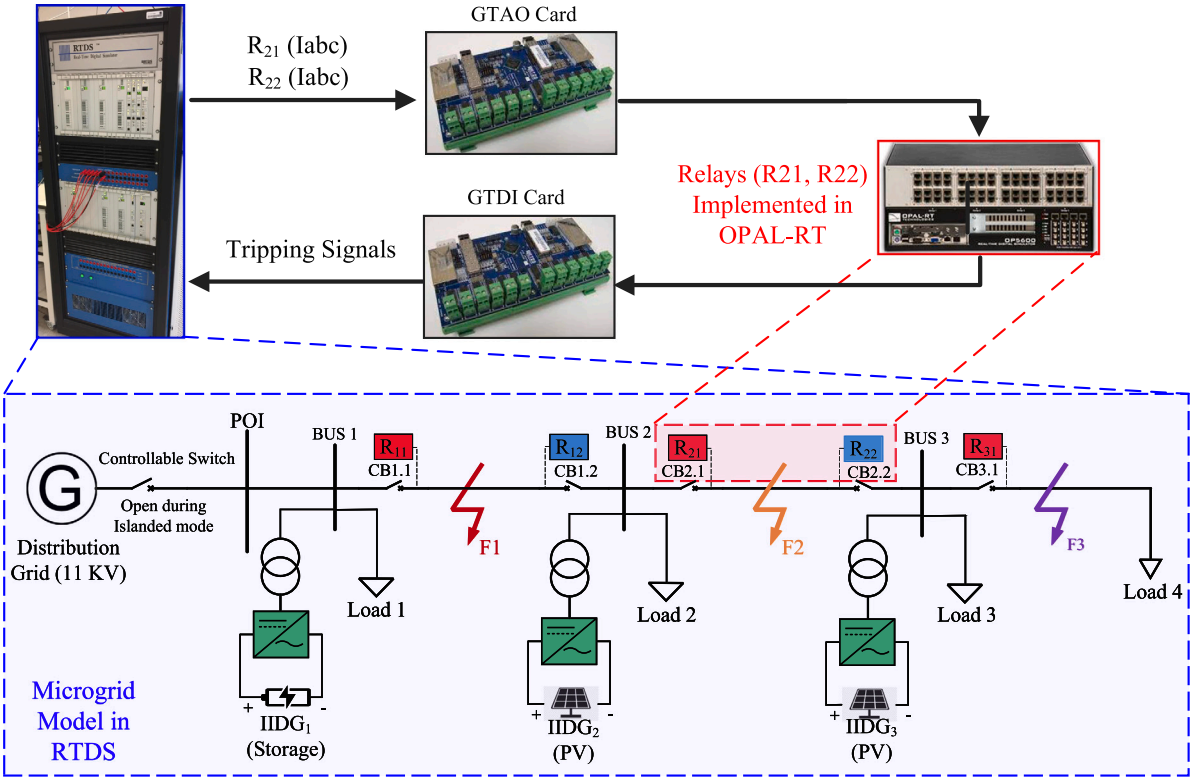

Fig. 11. HiL testing setup in laboratory.

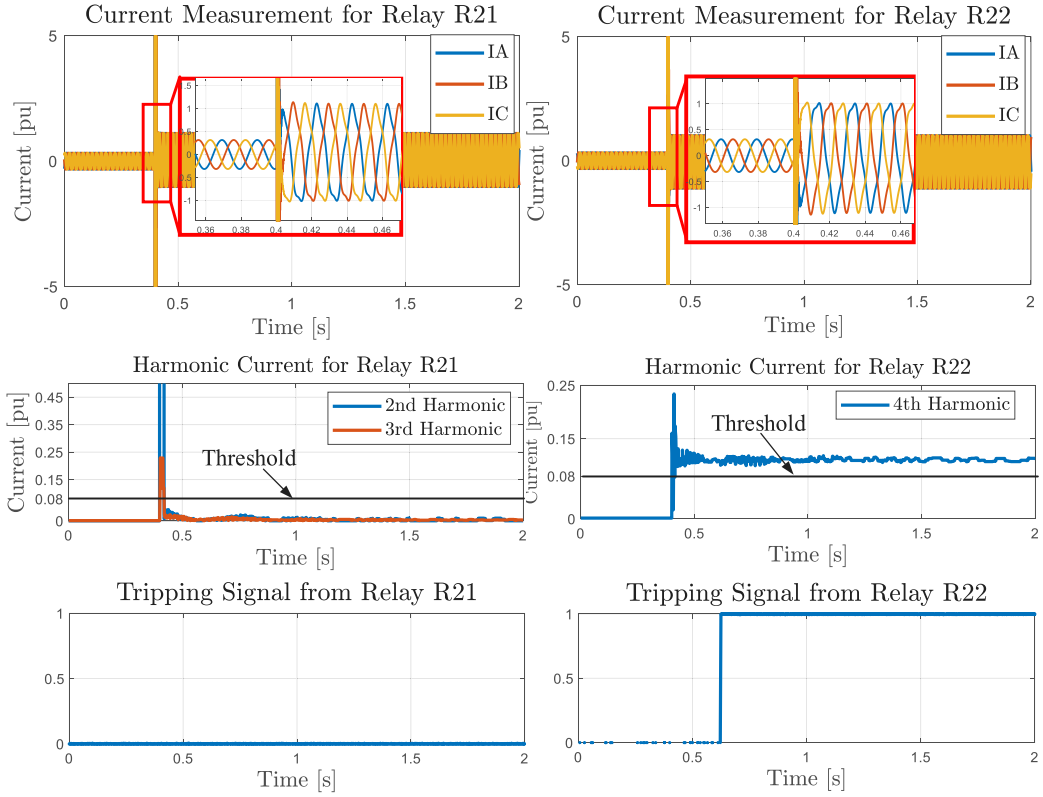

Fig. 12. HiL test results for a fault at F_1.

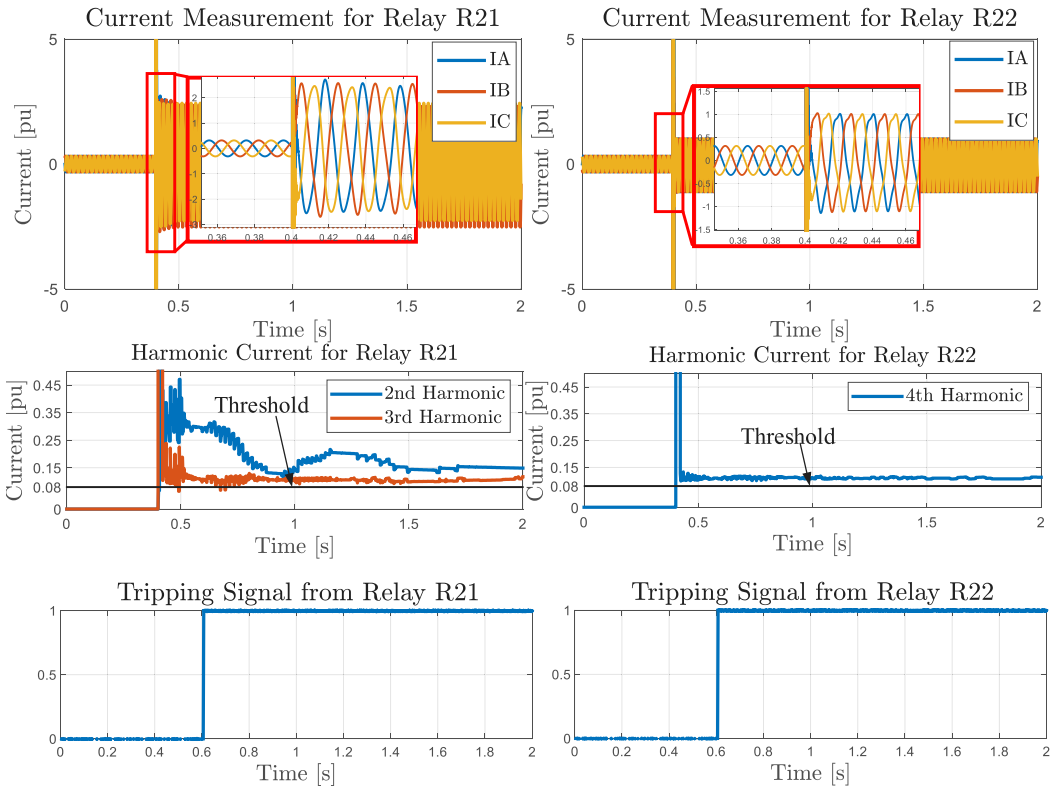

Fig. 13. HiL test results for a fault at F_2.

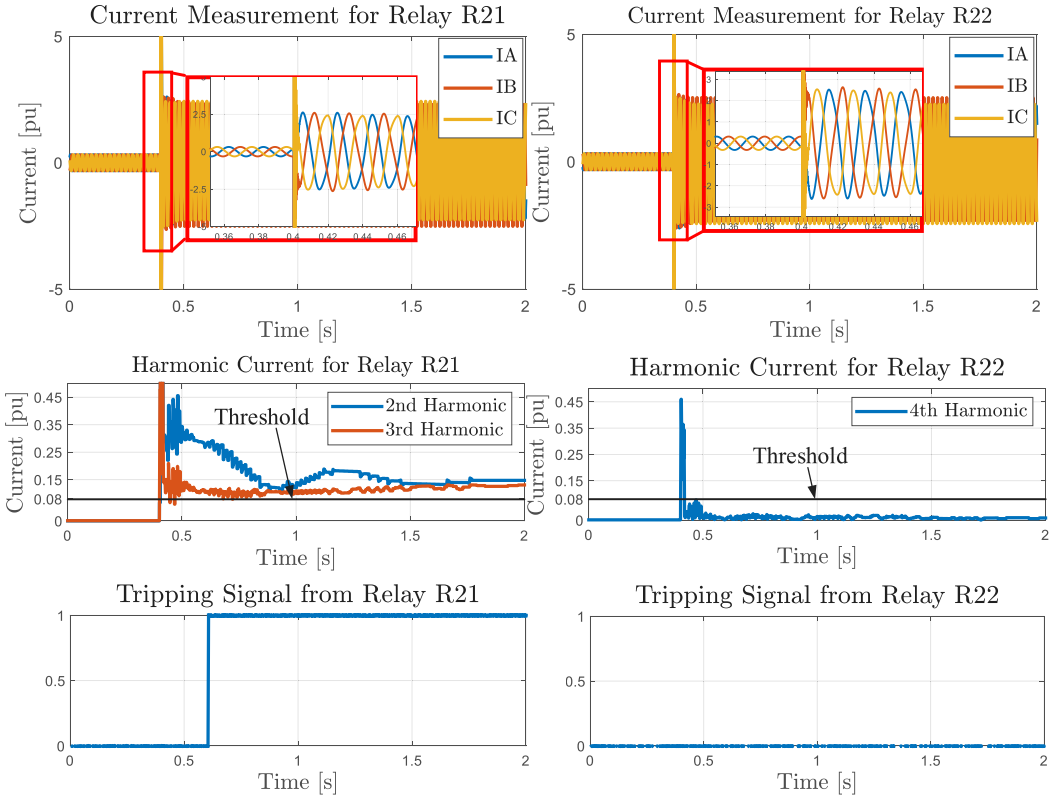

Fig. 14. HiL test results for a fault at F_3.

Table 5
Results of different combination of IIDG location with a three-phase fault at F_3.

Case No.	Connected generators			Fault clearing time				
	$IIDG_1$	$IIDG_2$	$IIDG_3$	CB1.1	CB1.2	CB2.1	CB2.2	CB3.1
41	On	Off	Off	0.8 s	–	0.7 s	–	0.6 s
42	On	On	Off	0.8 s	–	0.7 s	–	0.6 s
43	On	Off	On	0.8 s	–	0.7 s	–	0.6 s

challenges in islanded microgrids dominated by IIDGs. With the proposed protection method, the IIDGs are configured to inject specific harmonic components (which are different and for individual inverters) during fault conditions. A specific harmonic component with a magnitude of 10% (of fault current) is injected during the fault by each inverter. The relays in the network detect and isolate the faults, based on the harmonic analysis of the recorded current signals. A wide range of fault scenarios have been tested and demonstrated, including varying location and type of faults, varying line and fault impedance, testing for different combinations of connections of IIDGs with and without connection of SG. The scheme operates correctly for all tested scenarios.

Future work should include further investigation of practical implementation and application of the proposed scheme, in order to ascertain real world performance, the limits (e.g. in terms of the number of inverters/generators that can be used in a system), possible issues associated with harmonic limits/interference/resonance. Furthermore, investigation into how the fault detection methods employed in the IIDG controller may be optimised or improved will be undertaken. This could include using different logical combination of low voltage, unbalance/negative/zero sequence currents and rate of change of voltage to achieve the optimal balance between dependability and security of the proposed scheme.

CRediT authorship contribution statement

Md Asif Uddin Khan: Conceptualisation, Methodology, Software, Validation, Formal analysis, Investigation, Visualisation, Data curation, Writing – original draft, Writing – review & editing. **Qiteng Hong:** Conceptualisation, Formal analysis, Writing – review & editing, Visualisation, Supervision. **Agustí Egea-Àlvarez:** Writing – review & editing, Visualisation. **Adam Dyśko:** Conceptualisation, Writing – review & editing, Supervision. **Campbell Booth:** Conceptualisation, Writing – review & editing, Visualisation, Supervision, Project administration.

Declaration of competing interest

The authors declare that they have no known competing financial interests or personal relationships that could have appeared to influence the work reported in this paper.

Acknowledgment

This research is supported by the Engineering and Physical Sciences Research Council (EPSRC) in the UK via the Resilient Future Urban Energy Systems Capable of Surviving in Extreme Events (RESCUE) project [Grant Number: EP/T021829/1].

References

[1] Legislation. Climate change act 2008. London: UK Government; 2021, [Online]. Available: https://www.legislation.gov.uk/ukpga/2008/27/data.pdf.
[2] Committee on Climate Change. Net zero: Technical report. Tech. rep., London, United Kingdom; 2019, https://www.theccc.org.uk/publication/net-zero-technical-report/.
[3] Hatziargyriou N, Asano H, Iravani R, Marnay C. Microgrids. IEEE Power and Energy Magazine 2007;5(4):78–94.
[4] Barnes M, Kondoh J, Asano H, Oyarzabal J, Ventakaramanan G, Lasseter R, Hatziargyriou N, Green T. Real-world microgrids-an overview. In: 2007 IEEE International Conference on System of Systems Engineering. 2007, p. 1–8.
[5] Khan MAU, Hong Q, Liu D, Alvarez AE, Dyśko A, Booth C, Rostom D. Comparative evaluation of dynamic performance of a virtual synchronous machine and synchronous machines. In: The 9th Renewable Power Generation Conference (RPG Dublin Online 2021). 2021, p. 366–71.
[6] Hooshyar A, Iravani R. Microgrid protection. Proceedings of the IEEE 2017;105(7):1332–53.
[7] IEEE Standards Coordinating Committee 21. IEEE application guide for IEEE std 1547(TM), IEEE standard for interconnecting distributed resources with electric power systems. In: IEEE Std 15472-2008. 2009, p. 1–217.
[8] Shuai Z, Shen C, Yin X, Liu X, Shen ZJ. Fault analysis of inverter-interfaced distributed generators with different control schemes. IEEE Transactions on Power Delivery 2018;33(3):1223–35.
[9] Khan MAU, Hong Q, Dyśko A, Booth C, Wang B, Dong X. Evaluation of fault characteristic in microgrids dominated by inverter-based distributed generators with different control strategies. In: 2019 IEEE 8th International Conference on Advanced Power System Automation and Protection (APAP). 2019, p. 846–9.
[10] Khan MAU, Hong Q, Dyśko A, Booth C. Performance analysis of the overcurrent protection for the renewable distributed generation dominated microgrids. In: 2020 IEEE Region 10 Symposium (TENSYMP). 2020, p. 1490–3.
[11] Khan MAU, Hong Q, Dyśko A, Booth C. Review and evaluation of protection issues and solutions for future distribution networks. In: 2019 54th International Universities Power Engineering Conference (UPEC). 2019, p. 1–6.
[12] Zamani MA, Yazdani A, Sidhu TS. A communication-assisted protection strategy for inverter-based medium-voltage microgrids. IEEE Transactions on Smart Grid 2012;3(4):2088–99.
[13] Nikolaidis VC, Papanikolaou E, Safigianni AS. A communication-assisted overcurrent protection scheme for radial distribution systems with distributed generation. IEEE Transactions on Smart Grid 2016;7(1):114–23.
[14] Sortomme E, Venkata SS, Mitra J. Microgrid protection using communication-assisted digital relays. IEEE Transactions on Power Delivery 2010;25(4):2789–96.
[15] Gururani A, Mohanty SR, Mohanta JC. Microgrid protection using Hilbert-Huang transform based-differential scheme. IET Generation, Transmission and Distribution 2016;10(15):3707–16.
[16] Li X, Dyśko A, Burt GM. Traveling wave-based protection scheme for inverter-dominated microgrid using mathematical morphology. IEEE Transactions on Smart Grid 2014;5(5):2211–8.
[17] Al-Nasseri H, Redfern M, Li F. A voltage based protection for micro-grids containing power electronic converters. In: 2006 IEEE Power Engineering Society General Meeting. 2006, p. 7 pp..
[18] Al-Nasseri H, Redfern MA. Harmonics content based protection scheme for micro-grids dominated by solid state converters. In: 2008 12th International Middle-East Power System Conference. 2008, p. 50–6.
[19] Coffele F, Booth C, Dyśko A. An adaptive overcurrent protection scheme for distribution networks. IEEE Transactions on Power Delivery 2015;30(2):561–8.
[20] Che L, Khodayar ME, Shahidehpour M. Adaptive protection system for microgrids: protection practices of a functional microgrid system.. IEEE Electrification Magazine 2014;2(1):66–80.
[21] Brahma S, Girgis A. Development of adaptive protection scheme for distribution systems with high penetration of distributed generation. In: 2003 IEEE Power Engineering Society General Meeting (IEEE Cat. No.03CH37491). 4, 2003, p. 2083–2083.
[22] Soleimanisardoo A, Kazemi Karegar H, Zeineldin HH. Differential frequency protection scheme based on off-nominal frequency injections for inverter-based islanded microgrids. IEEE Transactions on Smart Grid 2019;10(2):2107–14.
[23] Soleimanisardoo A, Kazemi Karegar H. Alleviating the impact of DGs and network operation modes on the protection system. IET Generation, Transmission and Distribution 2020;14(1):21–8.
[24] Chen Z, Pei X, Yang M, Peng L, Shi P. A novel protection scheme for inverter-interfaced microgrid (iim) operated in islanded mode. IEEE Transactions on Power Electronics 2018;33(9):7684–97.
[25] He X, Wang R, Wu J, Li W. Nature of power electronics and integration of power conversion with communication for talkative power. Nature Communication 2020;11(1):2479.
[26] Khan MAU, Hong Q, Dyśko A, Booth C. An active protection scheme for islanded microgrids. In: 15th International Conference on Developments in Power System Protection (DPSP 2020). 2020, p. 1–6.
[27] Rocabert J, Luna A, Blaabjerg F, Rodríguez P. Control of power converters in ac microgrids. IEEE Transactions on Power Electronics 2012;27(11):4734–49.
[28] IEEE Standards Corrdinating Committee 21. IEEE standard for the specification of microgrid controllers. In: IEEE Std 20307-2017. 2018, p. 1–43.
[29] National Grid. The serviced grid code- issue 5 revision 22. (4031152):2018, p. 1–3.
[30] Liserre M, Blaabjerg F, Hansen S. Design and control of an LCL-filter-based three-phase active rectifier. IEEE Transactions on Industry Applications 2005;41(5):1281–91.
[31] IEEE recommended practice and requirements for harmonic control in electric power systems. In: IEEE Std 519-2014 (Revision of IEEE Std 519-1992). 2014, p. 1–29.
[32] Peng C, Husain I, Huang AQ, Lequesne B, Briggs R. A fast mechanical switch for medium-voltage hybrid dc and ac circuit breakers. IEEE Transactions on Industry Applications 2016;52(4):2911–8.

[33] Haggis T, EON. Network design manual. Tech. rep., United Kingdom: EON Central Networks; 2006, [Online]. Available: https://www.yumpu.com/en/document/read/8953808/network-design-manual-eon-uk.

[34] RTDS Technologies. RTDS simulator hardware. Winnipeg, Canada; 2011, [Online]. Available: https://manualzz.com/doc/25744342/rtds-simulator-hardware.

[35] OPAL-RT Teachnologies. OPAL-RT OP5600 V3 series manuals. Quebec, Canada; 2018, [Online]. Available: https://www.manualslib.com/products/Opal-Rt-Op5600-V3-Series-10349361.html.